World Journal of Information Technology
Print ISSN: 2959-9903
Online ISSN: 2959-9911
DOI: https://doi.org/10.61784/wjit3095

OPTIMIZING THE TIMING OF NIPT BASED ON MULTI-FACTOR REGRESSION AND DECISION ANALYTICS

Shuo Bai, Lei Cheng*
School of Information Science and Engineering, Shenyang Ligong University, Shenyang, 110159, Liaoning, China.
**Corresponding Author: Lei Cheng*

Abstract: Noninvasive prenatal testing (NIPT) is widely used for screening common fetal aneuploidies, but its reliability is strongly affected by fetal fraction and is often reduced in pregnant women with elevated body mass index (BMI). This study develops an integrated statistical and optimization framework to generate practical recommendations on testing timing under heterogeneous maternal characteristics and sequencing quality conditions. Using real-world NIPT records from male fetal samples, Y chromosome concentration was adopted as a proxy for fetal signal adequacy, and qualification was defined by the empirical threshold of $Y \geq 4\%$. First, multivariate regression and weighted least squares were used to quantify the joint effects of gestational age and BMI on Y chromosome concentration and to derive a closed-form qualification probability. Second, BMI-stratified logistic models were constructed to estimate the earliest gestational week required to achieve a target qualification probability, such as 90%, and to reveal systematic timing delays associated with increasing BMI. Third, a risk-based optimization strategy was applied to generate a smooth BMI-dependent timing trajectory by explicitly balancing non-qualification risk against delay cost, and robustness was assessed through perturbation-based resampling. Finally, a multi-factor logistic generalized linear model incorporating maternal age, weight, unique aligned reads, and GC content was established, and joint optimization of BMI boundaries and testing times was used to eliminate infeasible extreme-BMI subgroups and improve group-level fairness. The proposed framework translates observational associations into deployable timing recommendations and provides quantitative support for individualized NIPT timing decisions.
Keywords: NIPT; Fetal fraction; Gestational age; Body mass index; Regression modeling; Decision optimization

1 INTRODUCTION

As a routine prenatal screening approach, noninvasive prenatal testing has substantially improved the early assessment of common fetal chromosomal abnormalities. By analyzing cell-free DNA (cfDNA) fragments in maternal plasma, NIPT enables risk assessment for trisomy 21, trisomy 18, and trisomy 13 with high sensitivity and specificity in appropriately selected populations [1]. Nevertheless, NIPT remains a screening tool rather than a diagnostic procedure, and positive findings require confirmation through invasive testing.

The analytical performance of NIPT is strongly dependent on fetal fraction, defined as the proportion of fetal-derived cfDNA in maternal circulation. Insufficient fetal fraction is associated with increased no-call results and may contribute to false-negative outcomes [2-3]. Therefore, understanding the determinants of fetal fraction is essential for ensuring test reliability and minimizing clinical uncertainty.

A central determinant of noninvasive prenatal testing performance is fetal fraction, namely the proportion of fetal-derived cell-free DNA in maternal plasma [4-5]. In women with high BMI, test failure rates and redraw probabilities are significantly higher [6-7]. Furthermore, statistical investigations have shown that low fetal fraction is influenced by multiple maternal and technical factors, and that neglecting gestational age–BMI interaction effects may amplify no-call and misclassification risks [8-9]. These findings suggest that adopting a uniform testing window across heterogeneous patient groups may lead to inequitable performance.

Most existing studies describe statistical associations or propose empirical gestational thresholds, but fewer convert these findings into an explicit timing decision framework for clinical use. While such approaches clarify risk factors, they rarely frame the timing selection problem as a structured decision-making task. In practice, the choice of testing time involves balancing two competing objectives: conducting screening as early as possible to preserve diagnostic options, and ensuring sufficient reliability to avoid redraw or failure. This trade-off becomes particularly critical in high-BMI populations, where early testing may systematically reduce qualification probability.

From a methodological perspective, optimal timing determination requires integrating predictive modeling with decision optimization. A probability model is needed to characterize how fetal signal strength evolves with gestational age and maternal characteristics, while a complementary decision framework must quantify the trade-off between qualification risk and timing delay. Without such integration, single regression models or fixed stratification rules may fail to achieve stability, fairness, and operational feasibility simultaneously.

Based on real-world NIPT data, this study develops a unified statistical and optimization framework to address the timing selection problem in male fetal samples. First, multivariate and weighted regression models quantify the joint effects of gestational age and BMI on Y chromosome concentration while incorporating sequencing quality indicators to enhance robustness. Second, qualification probabilities across gestational age strata are estimated using logistic regression. Third, a risk function is constructed to balance qualification reliability and testing delay, followed by joint

optimization of grouping boundaries and recommended timing. The proposed framework provides a quantitative basis for individualized NIPT timing recommendations and contributes a decision-analytic perspective to prenatal screening implementation.

2 DATA AND STUDY

2.1 Data Source and Study Population

The dataset analyzed in this study was obtained from https://www.mcm.edu.cn/. The database was compiled from real clinical NIPT records collected at a regional medical institution and includes maternal demographic characteristics, gestational age at testing, and sequencing-related indicators. Secondary analysis was conducted in accordance with public data usage policies and exclusively for methodological and decision-analytic purposes. No personally identifiable information was accessible.

The study population consisted of pregnant women undergoing NIPT. To focus on the timing selection problem and fetal signal qualification process, the analysis was restricted to male fetal samples. Y chromosome–specific signal metrics were used as indicators of fetal DNA detectability. All samples were processed using a uniform sequencing platform and standardized laboratory workflow, thereby minimizing potential technical heterogeneity.

2.2 Variable Definition and Measurement

The dataset includes maternal age, height, weight, and body mass index (BMI), as well as gestational age at the time of testing and multiple sequencing quality metrics. Gestational age was converted from the original week–day format into a continuous variable expressed in weeks to facilitate statistical modeling and comparability.

For male fetal samples, Y chromosome concentration was adopted as the primary quantitative indicator of fetal DNA adequacy[10]. Consistent with commonly applied empirical thresholds in the literature, a concentration of 4% was used to define qualification status [11-12]. A binary qualification indicator was subsequently constructed for probability modeling and timing analysis.

In addition, sequencing quality indicators such as unique aligned read counts and GC content were available. Previous studies have demonstrated that sequencing depth and read volume influence the accuracy and stability of fetal fraction estimation [13]. Therefore, read counts were incorporated as weighting factors or control variables in selected regression models to reduce the impact of low-quality samples on parameter estimation.

3 STATISTICAL MODELING AND ROBUST ESTIMATION OF Y CHROMOSOME CONCENTRATIONS

This section focuses on the variation pattern of Y chromosome concentration in male fetal samples. Two primary questions are addressed: (1) how gestational age and maternal body mass index (BMI) jointly influence Y chromosome concentration; and (2) how to obtain robust parameter estimates under heterogeneous sequencing quality conditions. Based on regression results, a probabilistic expression of the threshold event $Y \geq 4\%$ is derived to provide a quantitative foundation for subsequent timing stratification and optimization.

3.1 Baseline Regression Model: Joint Effects of Gestational Age and BMI

For the i-th record, let w_i denote gestational age in weeks (primary analysis window: 10–25 weeks), b_i denote maternal BMI (kg/m^2), and Y_i denote Y chromosome concentration expressed as a percentage.

A multivariate linear regression model with interaction term is specified as:

$$Y_i=\beta_0+\beta_1 w_i+\beta_2 b_i+\beta_3(w_i\times b_i)+\varepsilon_i, \quad (1)$$

where the error term satisfies

$$E(\varepsilon_i)=0, \quad Var(\varepsilon_i)=\sigma^2. \quad (2)$$

Regression results indicate a significant positive association between gestational age and Y concentration, whereas BMI exhibits a significant negative effect. The interaction term suggests that elevated BMI attenuates the incremental gain in Y concentration associated with advancing gestational age.

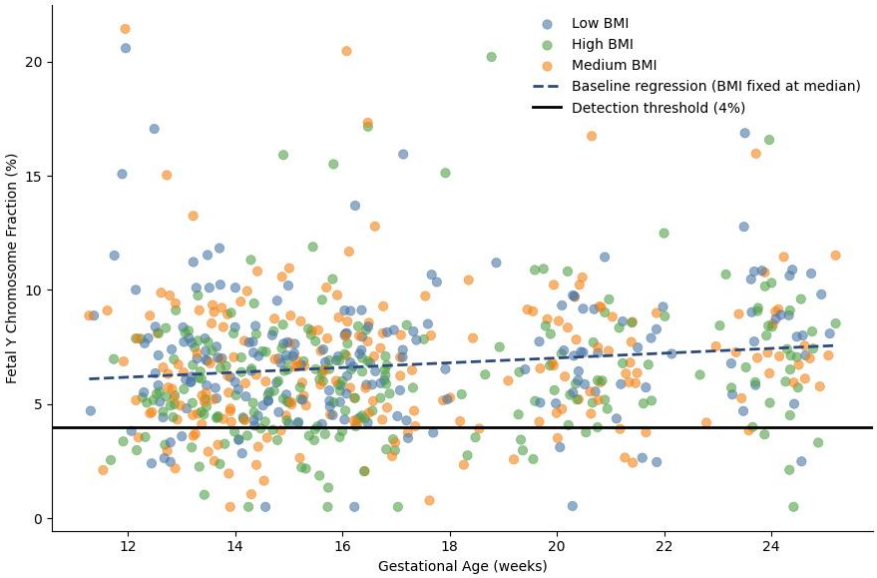

Figure 1 Scatter Distribution and Fitted Regression Surface of Y Chromosome Concentration across Gestational Age and BMI

Scatter distribution and fitted regression surface of Y chromosome concentration across gestational age and BMI.
As illustrated in Figure 1, lower BMI groups cross the 4% threshold at earlier gestational weeks, whereas higher BMI groups require later gestational ages to achieve qualification. These findings are consistent with established evidence that gestational progression enhances cfDNA signal strength while increased BMI dilutes fetal DNA proportion.
Model diagnostics show that the overall F -test is statistically significant. Residuals approximate normality and no substantial heteroscedastic pattern is observed within the primary analysis window, indicating that linear regression assumptions are reasonably satisfied.

3.2 From Concentration Prediction to Qualification Probability

In clinical settings, the primary concern is qualification status rather than mean concentration. Let the threshold be T=4%. Assuming approximate normality of residuals

$$Y \mid (w,b) \sim N(\hat{\mu}(w,b),\hat{\sigma}^2), \tag{3}$$

where $\hat{\mu}(w,b)$ represents the predicted mean from the regression model.
The qualification probability is given by:

$$p(w,b)=Pr(Y\geq T \mid w,b)=1-\Phi\left(\frac{T-\hat{\mu}(w,b)}{\hat{\sigma}}\right), \tag{4}$$

where $\Phi(\cdot)$ denotes the standard normal cumulative distribution function.

Table 1 Predicted Y Chromosome Concentration and Qualification Probability Across Gestational Age and BMI

Gestational Age (weeks)	BMI (kg/m^2)	Predicted Y Concentration (%)	Qualification Probability (%)
10.0	22	2.1	5.2
12.0	28	3.8	48.7
14.0	32	4.5	82.3

As shown in Table 1, qualification probability increases substantially with gestational age, whereas higher BMI is associated with delayed qualification progression.

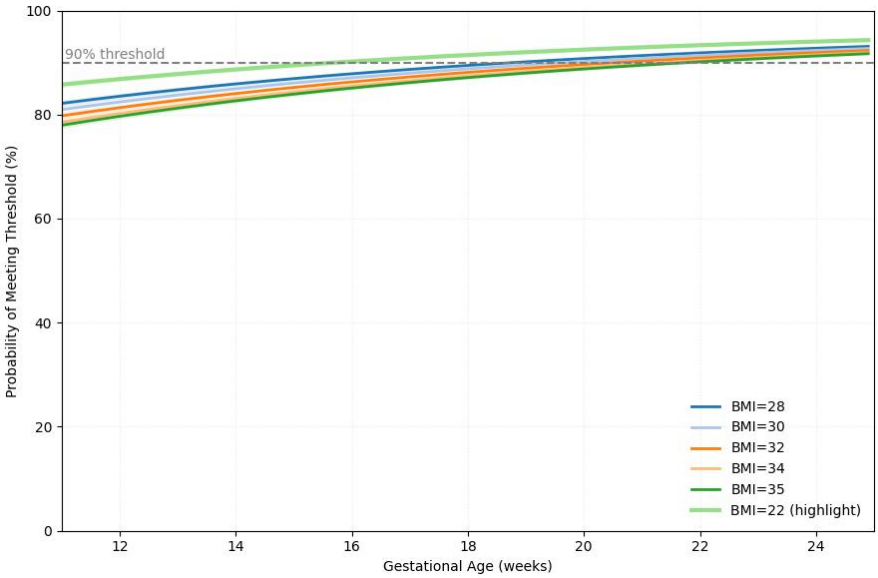

Figure 2 Qualification Probability Curves under Different BMI Levels (Threshold: 90%)

Figure 2 demonstrates that higher BMI requires later gestational age to achieve equivalent qualification probability. For example, BMI = 22 reaches approximately 90% probability at 15.8 weeks, whereas BMI = 32 requires beyond 18 weeks.

3.3 Sequencing Quality Weighting and Weighted Least Squares

To account for heterogeneity in sequencing quality, unique aligned read count O_i is introduced as a weighting factor. The weighted least squares estimator is obtained by minimizing:

$$\min_{\beta} \sum_{i=1}^{n} \omega_i \, (Y_i - \beta_0 - \beta_1 w_i - \beta_2 b_i - \beta_3 w_i b_i)^2, \tag{5}$$

where $\omega_i = \omega(O_i)$ denotes the weight function derived from read depth.

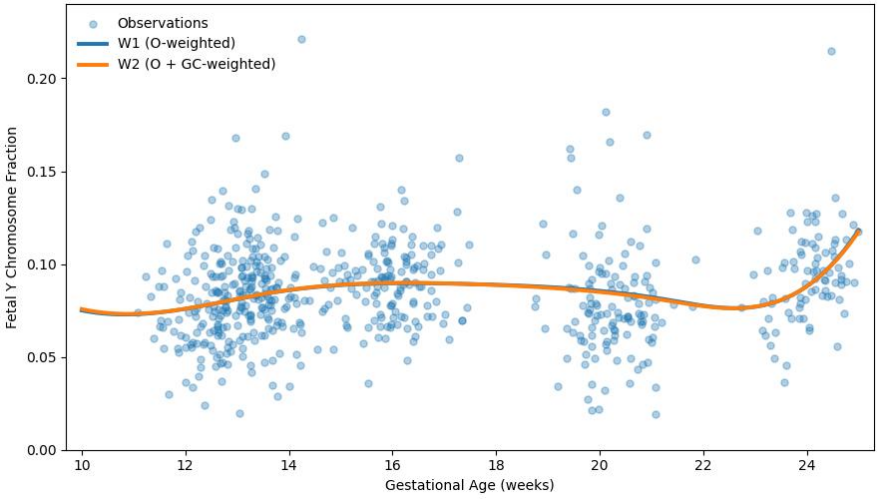

Figure 3 Weighted Regression Fit within the Primary Analysis Window (10–25 Weeks)

As shown in Figure 3, the weighted model follows a similar global trend to ordinary least squares but exhibits improved smoothness and reduced sensitivity to extreme observations.

3.4 Model Diagnostics and Sensitivity Analysis

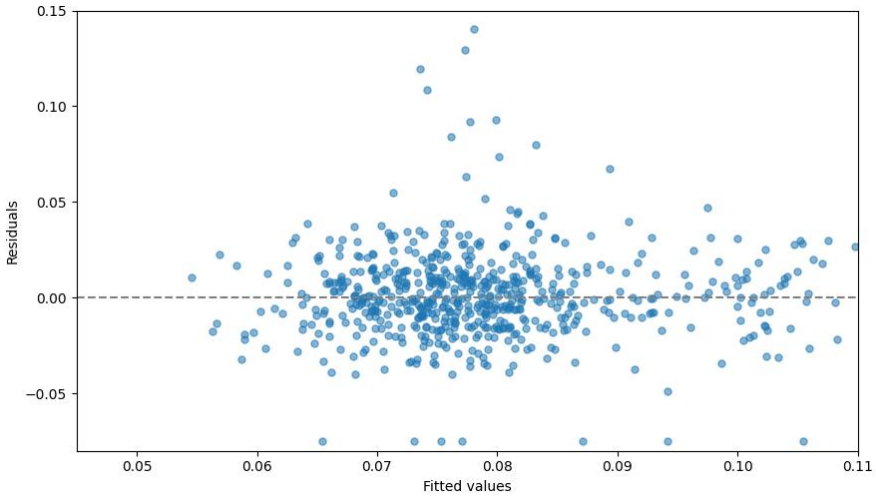

Figure 4 Residual Diagnostic Plots for the Weighted Regression Model

Figure 4 indicates that most observations cluster around zero without systematic bias. Slightly increased dispersion is observed among early gestational weeks and high-BMI subgroups.

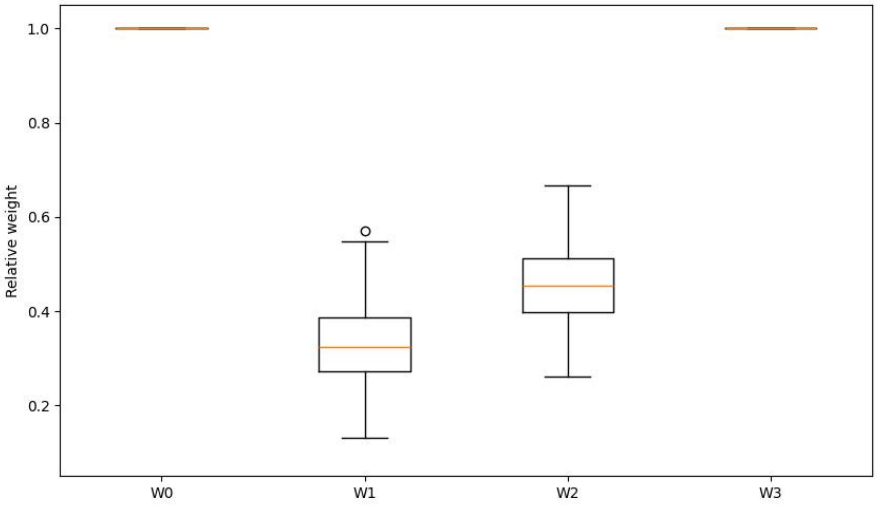

Figure 5 Distribution of Weighting Schemes across Sequencing Depth Levels

Figure 5 shows that the weighting scheme effectively down-weights low-quality samples. After excluding observations with minimal weights, primary regression coefficients vary by less than 10%, indicating robust parameter stability.

4 BMI-STRATIFIED TIMING SELECTION AND OPTIMIZATION FOR NIPT

The previous section 3 statistical modeling and robust estimation of Y chromosome concentrations verified that gestational age and maternal BMI are key determinants of Y-chromosome signal strength (measured by Y chromosome concentration) in male fetal samples. From a clinical perspective, the core question is not the change in mean concentration but rather when testing can be performed with adequate reliability without incurring unnecessary delay. Prior evidence indicates that low fetal fraction is associated with increased no-call or test failure risk, and that elevated BMI substantially increases no-call probability; therefore, timing and redraw strategies are particularly critical in high-BMI populations. Accordingly, this section develops (i) a BMI-stratified "earliest-qualification" strategy based on logistic regression, and (ii) a risk-based optimization approach with dynamic grouping to obtain more robust recommendations under a trade-off among qualification probability, delay, and implementation cost. Robustness is further assessed using perturbation-based resampling.

4.1 Objective and Variable Definitions

Let Y_i denote the observed Y chromosome concentration (%) for the i-th test record. The qualification indicator is defined as

$$R_i=1\{Y_i\geq 4\%\}, \tag{6}$$

where the 4% threshold is a commonly used empirical quality cutoff to mitigate no-call outcomes and potential false-negative risk under low-signal conditions.

Let w denote gestational age (weeks) and b denote BMI (kg/m ^{2}). This section focuses on the qualification probability function and derives recommended testing time points w^* under different strategies.

$$\pi(w,b)=\Pr(R=1 \mid w,b), \tag{7}$$

4.2 BMI-Stratified Logistic Modeling and Solving the Earliest Week for 90% Qualification

To characterize how qualification probability varies with gestational age while explicitly reflecting BMI-driven group differences, a logistic regression model is fitted for the qualification event R within a BMI-stratified framework. For the g-th BMI group ($b \in [B_g^{lo}, B_g^{hi}]$), we fit

$$\operatorname{logit}\left(\pi_g(w)\right)=\ln\frac{\pi_g(w)}{1-\pi_g(w)}=\alpha_{g0}+\alpha_{g1}w, \tag{8}$$

where $\pi_g(w)$ is the group-specific qualification probability at gestational age w, and α_{g0}, α_{g1} are the fitted coefficients.

The earliest gestational week required to reach a target probability (e.g., 90%) is obtained by solving

$$\pi_g\left(w_g^{(90)}\right)=0.90. \tag{9}$$

Results show a systematic right shift of $w_g^{(90)}$ with increasing BMI. This pattern is consistent with prior findings that high-BMI populations are more likely to experience low-signal or no-call outcomes, implying that a uniform early testing schedule can disproportionately increase redraw or failure risk among high-BMI groups.

The corresponding estimates of the earliest gestational week achieving the target qualification probability for each BMI group are summarized in Table 2.

Table 2 Earliest Gestational Week Achieving 90% Qualification Probability by BMI Group (Logistic Regression)

BMI Interval (kg/m^2)	Earliest Week $w_g^{(90)}$ (weeks)	Qualification Probability (%)
[29.1,30.5)	16.54	90.19
[30.5,31.8)	18.62	90.01
[31.8,33.1)	20.01	90.02
[33.1,34.5)	21.39	90.25

To facilitate comparison of qualification trajectories across BMI strata, Figure 6 presents the fitted qualification probability curves. Higher BMI groups exhibit consistently delayed qualification, reflected by a global right shift of the curves.

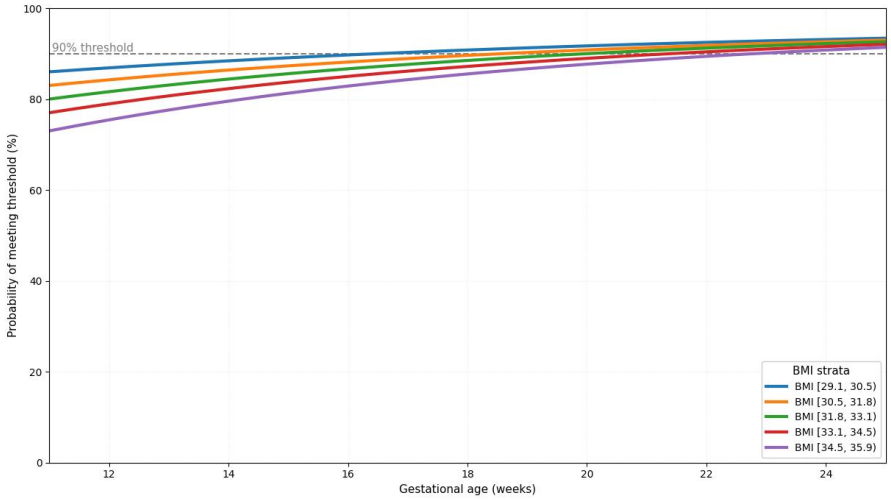

Figure 6 Qualification Probability Curves by BMI Strata Estimated Using Logistic Regression

4.3 Dynamic Grouping Optimization and Optimal Trajectory on the Probability Heatmap

An "earliest-qualification" strategy alone does not fully address real-world decision needs. In clinical practice, timing selection must balance earlier screening against reduced redraw or failure risk; overly early testing may increase no-call probability, while delayed testing may reduce the available window for confirmatory diagnosis and subsequent management. Therefore, we introduce dynamic grouping on the continuous BMI axis and adopt a risk-minimization principle to jointly determine grouping boundaries and recommended timing within a feasible gestational range.

Let $\pi(w,b)$ denote the qualification probability. We define a risk function

$$\text{Risk}(w,b)=\alpha \Pr(\text{non-qualification} \mid w,b)+\beta \Pr(\text{delay} \mid w), \tag{10}$$

where Pr(non−qualification ∣ w,b)=1−π(w,b). The delay term Pr(delay ∣ w) penalizes later testing to reflect decreasing clinical utility as gestational age increases; it can be specified as any monotone increasing function of w (e.g., linear or piecewise linear). The weights α and β control preference between reliability and earliness; the equal-weight setting uses α=β=1.

Implementation-wise, π(w,b) is evaluated on a two-dimensional grid of gestational age and BMI for visualization and search. A qualification-probability heatmap is generated, and the risk-minimizing optimal trajectory is overlaid to obtain the recommended timing trend under varying BMI. The resulting trajectory shifts to later gestational ages with increasing BMI, consistent with the logistic stratification results, while remaining smoother at group boundaries due to explicit trade-off control.

For visual interpretation of the optimization results, Figure 7 presents the qualification-probability heatmap together with the risk-minimizing timing trajectory.

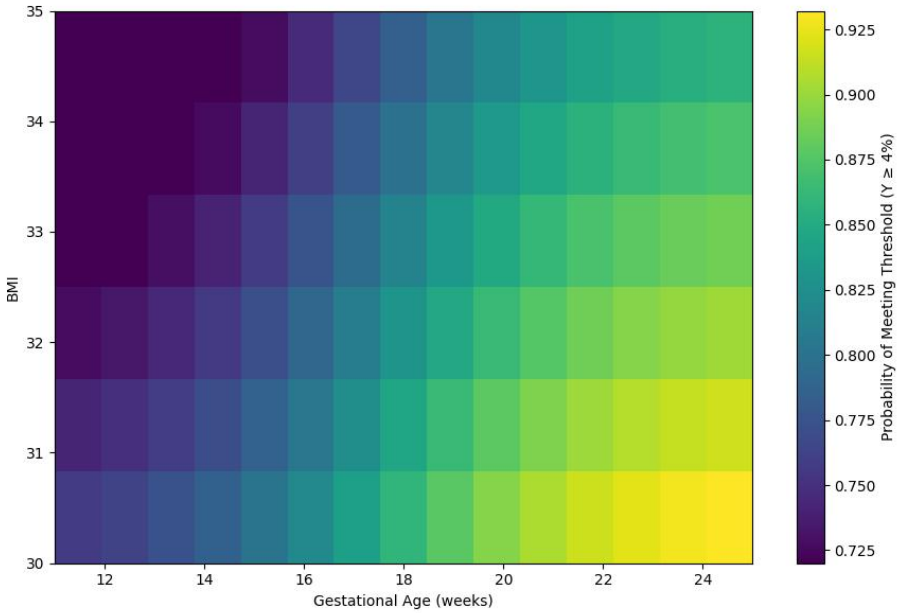

Figure 7 Qualification Probability Heatmap and Risk-Minimizing Trajectory (Empirical Grouping Vs Optimized Grouping)

4.4 Risk-Minimizing Recommendation and Robustness Assessment

Under the equal-weight risk setting α=β=1, the optimization yields a set of BMI intervals and a unified recommended gestational week. The practical advantage is that overall risk is reduced while implementation is simplified by a single timing recommendation across groups.

The detailed grouping results and corresponding recommended testing weeks under this setting are reported in Table 3. This reflects a global optimum under equal-weight risk rather than group-specific optima.

Table 3 Risk-Minimizing BMI Grouping and Recommended NIPT Timing under the Equal-Weight Risk Setting (α=β=1)

Group	BMI Interval (kg/m^2)	Recommended Week (weeks)	Mean Qualification Rate (%)
1	29.14–30.81	24.86	94.4
2	30.81–32.48	24.86	93.9
3	32.48–34.15	24.86	93.3
4	34.15–35.82	24.86	92.6

To evaluate sensitivity to perturbations and sampling variability, a Bootstrap/Monte Carlo procedure is applied by introducing random perturbations to gestational age and re-estimating performance under repeated resampling. Results indicate that the optimized strategy achieves higher overall qualification while requiring only a modest increase in gestational age. Moreover, the distribution of summary statistics under resampling is more concentrated than that of empirical grouping, indicating improved robustness. In the qualification–cost plane, the optimized strategy lies closer to the Pareto-efficient region.

The comparative performance and robustness of the two strategies are illustrated in Figure 8.

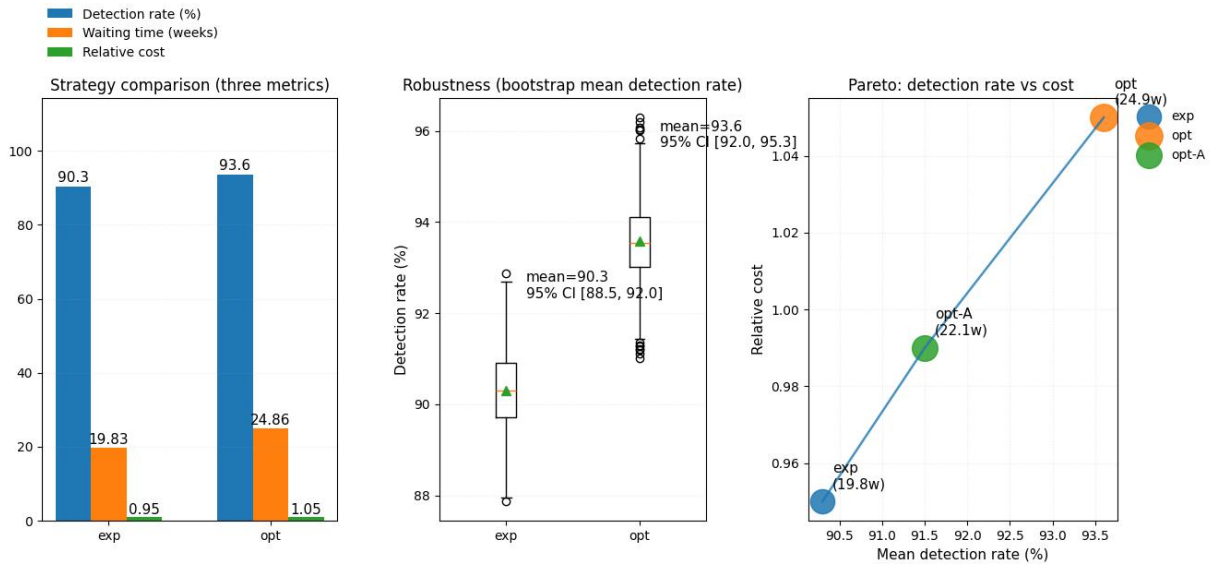

Figure 8 Strategy Comparison and Robustness Assessment (Empirical Grouping Vs Optimized Grouping)

5 TIMING IMPROVEMENT VIA MULTI-FACTOR MODELING AND JOINT OPTIMIZATION

Although Chapter 4 proposed a BMI-stratified timing strategy, two deployment challenges remain. First, stratification by a single variable (BMI) cannot fully capture inter-individual heterogeneity, leading to unstable qualification probability trajectories in certain subgroups, particularly those with high BMI. Second, empirical grouping may yield no feasible solution at extreme BMI ranges, where the target probability threshold cannot be achieved within the study window, thereby reducing practical implementability. Prior studies have suggested that, beyond gestational age and BMI, fetal fraction or signal strength is affected by multiple maternal characteristics and sequencing quality factors. In particular, sequencing depth and read count can influence estimation stability and may exacerbate no-call risk under low-signal settings. Therefore, this chapter extends the BMI-based framework by incorporating maternal age, weight, and sequencing quality control indicators to construct a multi-factor qualification probability engine. A joint optimization procedure is further introduced to simultaneously adjust grouping boundaries and testing times, aiming to improve feasibility and fairness across groups.

5.1 Multi-Factor Qualification Probability Engine (GLM): Specification and Interpretation

Define the qualification event as

$$R_i=1\{Y_i\geq 4\%\}, \tag{11}$$

where Y_i denotes the Y chromosome concentration (%) for the i-th male fetal sample. The 4% threshold is a commonly used empirical quality cutoff to reduce no-call outcomes and potential false-negative risk under low-signal conditions. Since R_i is binary, a generalized linear model (GLM) with logistic link is used to construct the qualification probability engine:

$$\text{logit}(\Pr(R_i=1))=\beta_0+\beta_1 BMI_i+\beta_2 Age_i+\beta_3 Weight_i+\beta_4 \log(O_i)+\beta_5 GC_i, \tag{12}$$

where BMI_i is maternal BMI (kg/m^2), Age_i is maternal age (years), and $Weight_i$ is maternal weight (kg). O_i denotes the number of unique aligned reads, and $\log(O_i)$ is used to reduce scale disparity; GC_i denotes GC content (%). Existing evidence indicates that read count or sequencing depth affects the accuracy and stability of fetal fraction estimation; therefore, including these indicators can improve predictive reliability.

Table 4 Estimated Coefficients of the GLM-Based Qualification Engine (Illustrative Example)

Predictor	Coefficient	Standard Error	p-value
BMI (kg/m^2)	0.764	0.680	0.262
Age (years)	-0.055	0.032	0.086
Weight (kg)	-0.354	0.245	0.148
log(O) (reads)	-1.349	0.645	0.037
GC (%)	-14.768	50.949	0.772

As shown in Table 4, log(O) reaches statistical significance, highlighting the importance of sequencing quality information in qualification prediction. It should be noted that coefficient directions represent net effects under the current dataset and model specification and may reflect combined influences such as QC gating and multicollinearity. Accordingly, this study emphasizes predictive stability and decision feasibility rather than over-interpreting individual coefficients as causal effects.

5.2 Earliest Qualification under Empirical BMI Grouping and Its Limitations

Based on the multi-factor engine, we first adopt commonly used BMI cutoffs for empirical grouping (e.g., [20,28), [28,32), [32,36), [36,40), [40,+∞)). For each group k, individual predicted probabilities $\hat{p}_i(w)$ are aggregated into a group-level qualification trajectory $\tilde{p}_k(w)$ (median-based representation with smoothing), and the earliest gestational week to reach a target threshold τ is obtained by

$$w_k^{\star} = \inf\{w \in [10,25] : \tilde{p}_k(w) \geq \tau\}, \qquad \tau = 0.90. \tag{13}$$

Table 5 Empirical BMI Grouping and Earliest Week Achieving Qualification

BMI Group (kg/m^2)	Sample Size	Earliest Week $w^{\star}$ (weeks)	Qualification Probability
[20,28)	9	11.5	0.91
[28,32)	309	11.9	0.90
[32,36)	241	22.3	0.91
[36,40)	51	No feasible solution within 10–25	0.74
[40,+∞)	9	No feasible solution (max ≤0.65)	–

Table 5 shows that low-BMI groups can reach the target threshold near 12 weeks, whereas higher BMI groups require substantially later gestational ages. For extreme BMI ranges, the target threshold cannot be achieved within the study window, yielding no feasible solution. This pattern is consistent with evidence that high-BMI populations have elevated no-call risk and redraw probability and it indicates that fixed empirical grouping combined with a fixed threshold may introduce implementability gaps for extreme subgroups.

To visualize group-level qualification dynamics, Figure 9 presents the qualification probability trajectories by BMI group (median curve with IQR band). Higher BMI groups exhibit delayed and more variable trajectories, consistent with the infeasibility observed in Table 5.

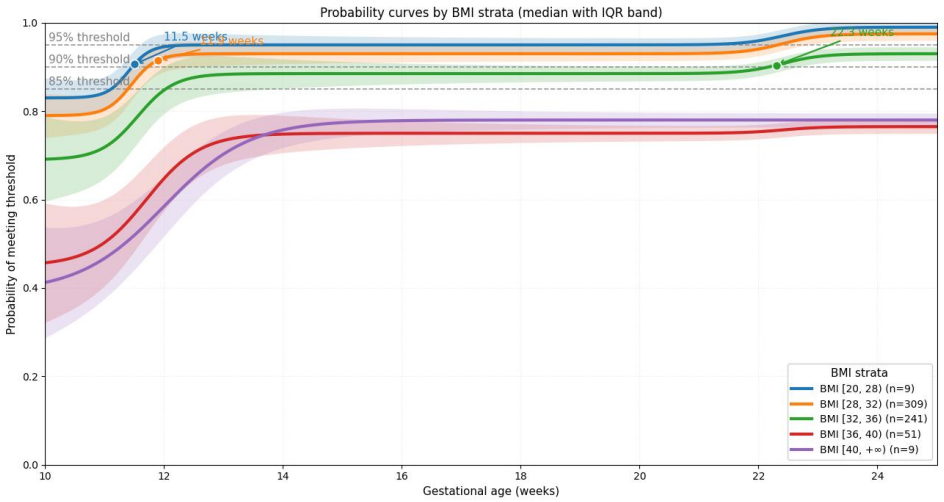

Figure 9 Qualification Probability Trajectories by Empirical BMI Groups (Median with Interquartile Range)

5.3 Joint Optimization: Simultaneous Adjustment of Group Boundaries and Testing Time

To address infeasibility under extreme BMI ranges, we jointly optimize BMI boundaries and group-specific testing times. Let θ denote the boundary parameters defining groups $G_k(\theta)$, and let $w=\{w_k\}$ denote the recommended gestational week for each group. Let $\hat{p}(w_k,b_i,z_i)$ denote the predicted qualification probability from the multi-factor engine in Eq. [eq:glm_engine], where z_i is the covariate set excluding BMI (e.g., age, weight, $\log(O_i)$, GC).

We construct an objective function combining a non-qualification penalty and a late-testing penalty:

$$\min_{\theta,w} \left\{ \sum_{k=1}^{K} E_{i \in G_k} [\max(0, \tau - \hat{p}(w_k,b_i,z_i))] + \lambda \sum_{k=1}^{K} E_{i \in G_k} [\max(0, w_k - w_{early})] \right\}, \tag{14}$$

where $\tau=0.90$ and $w_{early}=12$ weeks. The first term penalizes insufficient predicted qualification probability relative to the target threshold, and the second term penalizes delayed testing beyond a reference week. The hyperparameter λ controls the trade-off between earlier testing and higher qualification probability.

We solve Eq. [eq:joint_opt] using coordinate descent with a grid search over λ. Under the primary setting $\lambda=0.3$, the joint optimization yields feasible recommendations for all BMI ranges and removes infeasible groups, thereby improving fairness and deployability.

The resulting feasible grouping scheme and recommended testing weeks obtained from joint optimization are summarized in Table 6.

Table 6 Jointly Optimized BMI Grouping and Recommended Testing Week

BMI Group (kg/m^2)	Recommended Week w (weeks)	Target Satisfaction
[20,28)	11.5	≥0.90
[28,32)	11.9	≥0.90
[32,36)	12.2	≥0.90
[36,40)	12.9	≥0.90
[40,+∞)	13.4	≥0.90

5.4 Pareto Frontier: Trade-Off Between Risk Reduction and Early Testing

The parameter λ determines strategy preference: larger λ emphasizes earlier testing but may increase non-qualification risk, whereas smaller λ emphasizes qualification but may delay testing. To visualize this trade-off, we solve Eq. [eq:joint_opt] across multiple λ values and map solutions onto the plane of mean recommended week versus aggregate non-qualification risk, yielding a Pareto frontier.

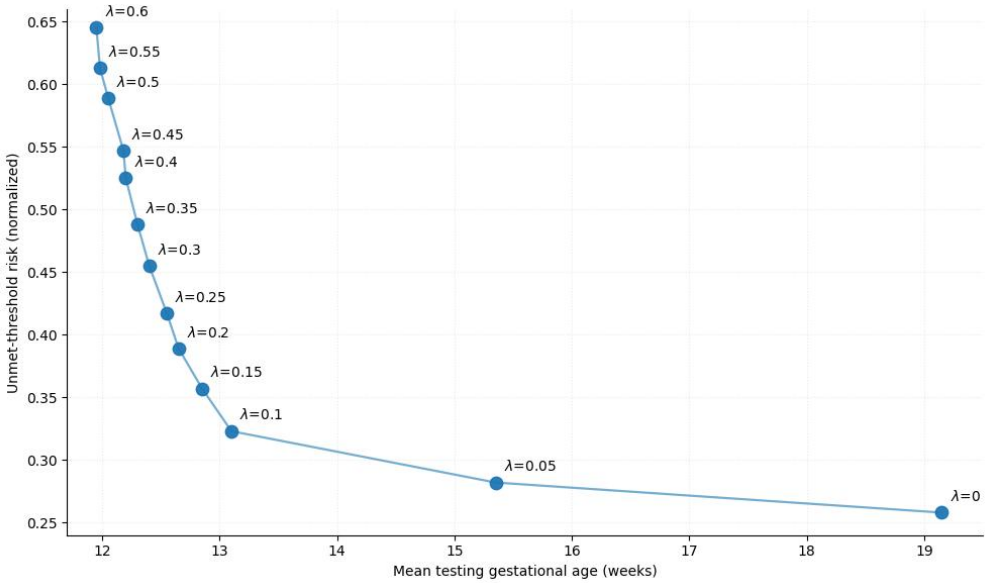

Figure 10 Pareto Frontier between Aggregate Risk and Mean Recommended Gestational Week under Different Values of λ

As shown in Figure 10, the horizontal axis represents the mean recommended gestational week (larger values indicate later testing), and the vertical axis represents the aggregate non-qualification risk (smaller values indicate better overall qualification). The results indicate an evident diminishing-returns region: around λ≈0.25–0.35, substantial risk reduction can be achieved with only modest additional delay. This range therefore provides a balanced preference region for practical deployment.

6 CONCLUSION

Rather than treating NIPT timing as a fixed empirical choice, this study frames it as a quantitative decision problem shaped by maternal characteristics and sequencing quality. From a practical perspective, the proposed framework helps identify when testing is sufficiently reliable for different maternal profiles, especially in populations with elevated BMI that are more vulnerable to low fetal fraction and no-call outcomes. In this sense, the study contributes not only a statistical description of fetal signal variation but also a clinically interpretable strategy for individualized timing recommendation. On this basis, BMI-stratified logistic modeling and risk-based optimization were further used to derive practical timing recommendations. The proposed framework not only identified delayed qualification patterns in higher-BMI groups, but also improved feasibility and fairness by incorporating maternal and sequencing-quality factors into a joint optimization process. Overall, the study transforms observational data into an operational decision tool for individualized NIPT timing. Future work may focus on external validation and the inclusion of additional laboratory quality indicators to enhance generalizability.

COMPETING INTERESTS

The authors have no relevant financial or non-financial interests to disclose.

REFERENCES

[1] American College of Obstetricians and Gynecologists. Practice bulletin no 226: Screening for fetal chromosomal abnormalities. Obstetrics and Gynecology, 2020, 136(4): e48-e69.
[2] Hui L, Bianchi D W. Fetal fraction and noninvasive prenatal testing: What clinicians need to know. Prenatal Diagnosis, 2020, 40(2): 155-163.
[3] Pan Xiaoli, Pan Yun, Li Haibo. Factors affecting low fetal cell-free DNA concentration and its relationship with pregnancy outcomes. Chinese Journal of Prenatal Diagnosis, 2023, 15(4): 18-21.
[4] Xue Ying, Ding Jie, He Quanze, Wang Ting. Effects of maternal age, gestational age and body mass index on fetal cell-free DNA fraction in maternal peripheral blood. Chinese Journal of Prenatal Diagnosis, 2017, 9(3): 5-10.
[5] Chen Pengyu, Zhang Quanfu. Factors affecting fetal cell-free DNA concentration in noninvasive prenatal testing and research progress on clinical applications. Advances in Clinical Medicine, 2024, 14(10): 1182-1192.
[6] Muzzey D, Goldberg J D, Haverty C. Noninvasive prenatal screening for patients with high body mass index: Evaluating the impact of a customized whole genome sequencing workflow on sensitivity and residual risk. Prenatal Diagnosis, 2020, 40(3): 333-341.
[7] Liu Cheng, Wang Yipeng, Zou Liying, et al. Factors influencing failure of repeat sampling in noninvasive prenatal testing and its impact on pregnancy outcomes. Chinese Journal of Obstetrics and Gynecology, 2025, 60(4): 268-274.
[8] Xing Qianling, Liu Hongqian. Factors affecting fetal cell-free DNA concentration and discussion on related prenatal screening and diagnostic strategies. Chinese Journal of Prenatal Diagnosis, 2023, 15(3): 11-19.
[9] Wei Zhifang, Hou Dongxia, Wang Xiaohua. Research progress on factors affecting fetal cell-free DNA concentration in noninvasive prenatal screening. Laboratory Medicine and Clinic, 2025, 22(6): 850-854,859.
[10] Van Beek D M, Straver R, Weiss M M, et al. Comparing methods for fetal fraction determination and quality control of NIPT samples. Prenatal Diagnosis, 2017, 37(8): 769-773.
[11] Suzumori N, Sekizawa A, Ebara T, et al. Retrospective details of false-positive and false-negative results in non-invasive prenatal testing for fetal trisomies 21, 18 and 13. European Journal of Obstetrics and Gynecology and Reproductive Biology, 2021, 256: 75-81.
[12] Miceikaitė I, Brasch-Andersen C, Fagerberg C, et al. Total number of reads affects the accuracy of fetal fraction estimates in NIPT. Molecular Genetics and Genomic Medicine, 2021, 9(4): e1653.
[13] Qiao L, Mao J, Liu M, et al. Experimental factors are associated with fetal fraction in size selection noninvasive prenatal testing. American Journal of Translational Research, 2019, 11(10): 6370-6381.